Interference with *Fatty Acyl-CoA Reductase* Reduces Wax Secretion and Influences the Development of Male *Ericerus pela* (Hemiptera: Coccoidae) Nymphs[1]

Yanhong Hu, Heng Dong, Jiejun Zhao[2], and Linkai Cui[3]

College of Forestry, Henan University of Science and Technology, Luoyang, China

J. Entomol. Sci. 60(3): 000–000 (Month 2024)
DOI: 10.18474/JES24-59

Abstract *Ericerus pela* Chavannes (Hemiptera: Coccoidae) is a typical scale insect that can secrete a waxy covering over its body to protect itself from adverse factors. This insect significantly damages glossy privets and ash trees in most regions of China. The *fatty acyl-CoA reductase* (FAR) gene is a crucial enzyme in the cutin, suberine, and wax biosynthesis pathways in these insects and also in fatty acid metabolism. Herein, a synthesized double-stranded RNA of the *FAR* gene in *E. pela* (ds*EpFAR*) was used to explore the effects of ds*EpFAR* on the expression of *EpFAR* and secretion of wax and development of *E. pela*. The results showed that a high concentration of ds*EpFAR* could cause mortality of male nymphs. After a male nymph was treated with a low dose of ds*EpFAR*, the transcription level of *EpFAR* was significantly downregulated, the expression level of *EpFAR* protein was reduced, and the quantity of wax was markedly decreased, suggesting that *EpFAR* is a key gene in the biosynthesis of wax and that *dsEpFAR* can interfere with the gene *EpFAR* and disrupt the process of wax secretion. The growth and development of male nymphs were also significantly influenced by ds*EpFAR* treatment, leading to a significantly decreased weight and earlier nymph-to-pupae transition. The findings enhance the molecular understanding of male *E. pela* wax secretion and facilitate the development of *EpFAR*-based interference with wax secretion for the integrated management of male *E. pela*.

Key Words wax secretion, *fatty acyl-CoA reductase*, RNA interference

The white wax insect *Ericerus pela* Chavannes (Hemiptera: Coccoidae) commonly occurs in southwestern China (Fig. 1). The male nymphs have no sclerotized cuticle and secrete wax, whereas the females have a hard cuticle and cannot secrete wax. The males comprise 90% of a population. As second-instar nymphs, males move from host plant leaves onto branches where they aggregate and begin to secrete wax that forms a confluent, uniform protective wax layer. Most females in the aggregation disperse individually and not as a group (Chen 2011). In much of China, except southwestern China, this scale insect severely damages glossy privet shrubs and ash trees, leading to heavy economic losses as well as reduction in ornamental value and ecological function of the host plants (Wang and Wang 2014, Zhang and Guo 2018). *Ericerus pela* is managed primarily by the application of chemical insecticides. Because insecticides are known to harm

[1]Received 13 June 2024; accepted for publication 29 July 2024.
[2]Chinese Academy of Forestry Institute of Highland Forest Science, Kunming, China.
[3]Corresponding author (email: lyclk@163.com).

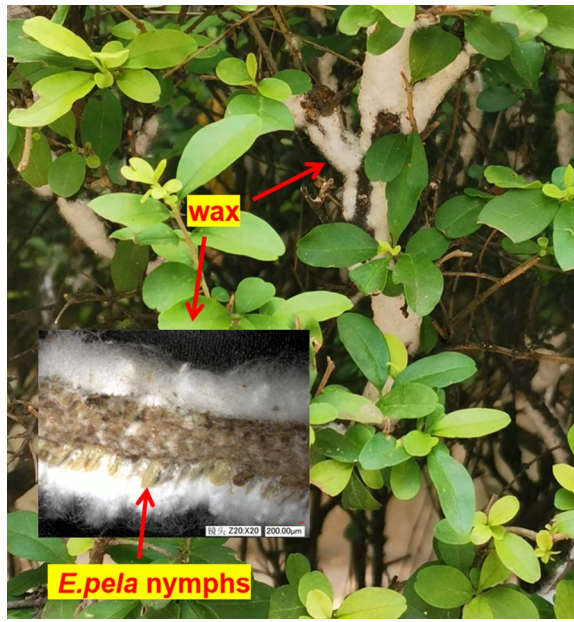

Fig. 1. Male *Ericerus pela* endangering glossy privet.

nontarget species and contaminate the environment, it is necessary to explore new species-specific agents as control methods (e.g., gene or gene products). Furthermore, because the wax secretions serve as a protective shield for male *E. pela* from insecticide applications, unveiling the function of genes associated with the biosynthesis of wax will be helpful in developing new management strategies for *E. pela*.

RNA interference (RNAi) is an effective posttranscriptional gene-silencing mechanism in eukaryotes and a powerful reverse genetic tool for functional genomic studies (Bellés 2010, Bosher and Labouesse 2000, Jain et al. 2020). Double-stranded RNA (dsRNA) is absorbed through the somatic or midgut cells of insects and processed into small interfering RNAs (siRNAs) by the endoribonuclease Dicer. The siRNAs then bind the complementary mRNA to interfere with the translation process of the target gene (Palli 2014, Wynant et al. 2014). Several studies have uncovered some roles of the target genes by using RNAi and confirmed that RNAi-mediated pest control is a feasible and effective strategy for crop protection, with potential safety and specificity advantages (Dang et al. 2022, Tian et al. 2015, Wang et al. 2021a). For example, the genes *AsFAR* in *Adelphocoris suturalis* (Jakovlev) (Hemiptera: Miridae), *JHAMT* in *Leptinotarsa decemlineata* (Say) (Coleoptera: Chrysomelidae), and *IAP* and *SNF7* in *Anoplophora glabripennis* (Motschulsky) (Coleoptera: Cerambycidae), which play major roles in the growth, development, or reproduction of these pests, have been confirmed and the introduction of homologous dsRNA of these genes into the corresponding insect hosts caused some typical phenotypes of specific gene deficiency, such as decreased weight, precocious metamorphosis, changed microstructure of epicuticle layer, malformed shape, and cessation of oocyte development

(Dhandapani et al. 2020, Guo et al. 2018, Luo et al. 2017). Our question at the onset of this study was can a dsRNA influence the life cycle of a *E. pela* nymph or/and the wax biosynthesis of male nymphs?

To date, the molecular mechanism of wax biosynthesis is not fully understood, thereby making it very difficult to manage wax-secreting pests by limiting or destroying the wax. It is known that the biosynthesis of wax primarily occurs in two successive catalytic steps: first, the reduction of fatty acyl-CoA to fatty alcohol and second, the subsequent esterification of fatty acyl-CoA and fatty alcohol (Cheng and Russell 2004, Teerawanichpan and Qiu 2010). The *fatty acyl-CoA reductase* gene (*FAR*), which encodes the biosynthesis of fatty alcohols and lipids in animals, plants, and microorganisms, is a key gene during development of insects (Jaspers et al. 2014, Li et al. 2020, Munkajohnpong et al. 2020, Wang et al. 2018, 2021b). Tong et al (2022) reported that *FAR* in mealybug *Phenacoccus solenopsis* Tinsley influences wax biosynthesis. Ding et al. (2022) analyzed transcriptome data of *E. pela* and concluded that *FAR* genes are important catalytic enzymes of fatty acid metabolism. Our previous study (Hu et al. 2018) on *E. pela FAR* (*EpFAR*) revealed that *EpFAR* is highly expressed in the testes and wax glands of male nymphs and can catalyze the reduction of fatty acyl-CoA into fatty alcohol. Because the testis is unique to males and only male *E. pela* can secrete wax, we hypothesized that *EpFAR* is key to the development of male nymphs and potentially involved in the biosynthesis of wax.

In this study, a double-stranded *EpFAR* (ds*EpFAR*) was synthesized and used to interfere with *EpFAR* in male *E. pela* nymphs to identify a potential target gene and illustrate whether the silencing of the target gene can harm normal life processes of *E. pela* nymphs. Our findings demonstrated that *EpFAR* plays an essential role in the wax secretion and development of male *E. pela* nymphs and that ds*EpFAR* can lead to higher mortality when the concentration of ds*EpFAR* is high and to a developmental defect with a lower concentration. Therefore, *EpFAR* is an ideal candidate gene for future development as RNAi-mediated control of *E. pela*.

Materials and Methods

Insects. Female *E. pela* adults carrying masses of eggs were collected from glossy privet in a park in Luoyang City (longitude E 112°26′; latitude N 34°37′), China, and held in a shady dry environment. These female adults were assigned to different batches and placed in gauze bags. Next, these bags were hung on the branches of *Ligustrum lucidum* Ait., which would serve as the hosts for the *E. pela* nymphs. These hosts were grown under shade in an experimental field at the College of Forestry, Henan University of Science and Technology, Luoyang, China. Newly molted male nymphs, aged 1–2 d, that had moved onto *L. lucidum* branches and gathered into a group but had not begun to secrete wax were treated with reagent. Because individual nymphs measure only 0.77 mm long and 0.43 mm wide and immobilize themselves on the branch, we selected the coating method to treat them with the reagent.

Synthesis of ds*EpFAR*. The Simple Modular Architecture Research Tool (http://smart.embl.de/) was used to predict the functional domains of *EpFAR*. Gene-specific primers for the synthesis of ds*EpFAR* were designed using Primer Premier 6.0 software based on the conserved sequence and functional domains of

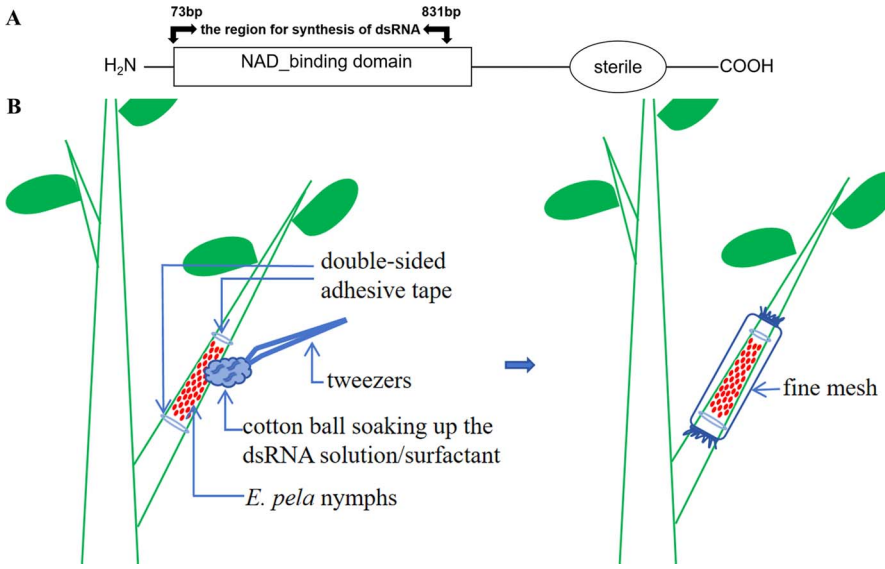

Fig. 2. Schematic illustration of the RNAi region (73–831 bp) in the conserved sequence and functional domains of the *Ericerus pela fatty acyl-CoA reductase* gene (A) and the method of treating the nymphs in this study (B).

EpFAR (Fig. 2A). The plasmid containing the *EpFAR* open reading frame prepared by Hu et al. (2018) was used as the template to amplify a 759-bp fragment by using gene-specific primers (Table 1). The amplification reactions were performed under the following conditions: predenaturation at 94°C for 4 min, followed by 32 cycles of denaturation at 94°C for 30 s, annealing at 55°C for 30 s, and extension

Table 1. Primers used in this study.

Primer	Primer Sequence*
For exogenous dsRNA synthesis	
ds*EpFAR*-F	*taatacgactcactatagggag*TTCGTTACAGGTGGAACAGG
ds*EpFAR*-R	*taatacgactcactatagggag*AACACTTCGCAACAACCCTA
For qRT-PCR	
EpFAR-F	TCACGCAGCAGCTACAGTAC
EpFAR-R	CTGATCTTATGGGTGGAGTGT
β-*actin*-F	GTGACGACGATGTTGCTGCTTTG
β-*actin*-R	CCCATGCCCACCATAATACCCTGAT

* Underlined sequences represent the T7 promoters.

at 72°C for 1 min by using a CFX96 polymerase chain reaction (PCR) system (Bio-Rad, Hercules, CA). The amplicons were purified using a PCR product recovery kit (SunShine Bio, Ltd., Shanghai, China). Next, approximately 1 μg of the recovered DNA per tube was used as the template to generate ds*EpFAR* by using a MEGAscript® RNAi kit (Invitrogen, Carlsbad, CA) according to the manufacturer's instructions. Finally, the concentration of ds*EpFAR* was measured by using a Thermo ND2000 spectrometer (Thermo Fisher Scientific, Waltham, MA).

Nontoxic dose of the surfactant screening. Triton X-100 (Sigma-Aldrich, St. Louis, MO) was used as a surfactant to make the solution of ds*EpFAR* uniformly adhere to the body of a nymph to facilitate ds*EpFAR* penetration through the cuticle. An effective and nontoxic dose of surfactant was screened first according our experimental program. Newly molted male nymphs on *L. lucidum* branches were treated with 3, 1, 0.3, 0.1, and 0.03% Triton X-100. Triton X-100 was coated on the body of nymphs by using a small piece of soft cotton. Next, double-sided adhesive tape was wrapped around the base of branches to inhibit untreated nymphs from joining the treated group; a fine mesh was used to shield the treated group from parasites or predators (Fig. 2B). The controls were treated with sterile water. The assay was conducted in three replicates. Each replicate of ≥30 nymphs was based on a group of male nymphs, given the gregarious life of male *E. pela*. The toxicity of Triton X-100 was assessed 5 d after treatment by determining the number of dead nymphs. Dead nymphs were identified based on color changes and detachment from their inhabiting sites when brushed with a soft hairbrush. A dose that caused no significantly different mortality from the control, and with excellent adhesion ability, was deemed as a nontoxic dose and used in follow-up assays.

Tolerated dose of ds*EpFAR* screening. To determine whether the ds*EpFAR* could lead to mortality, we investigated the effects of ds*EpFAR* on the lives of healthy nymphs. Triton X-100 is a nonionic detergent with the ability to improve the permeability of eukaryotic cell membrane in biological experiments, reduce the surface tension of ds*EpFAR* solution, and help ds*EpFAR* quickly adhere to the nymphal epidermis so as to be easily taken up through endocytosis. Based on the results from the aforementioned assay, a nontoxic dose of Triton X-100 was used as the surfactant. The concentrations of ds*EpFAR* used in the experiment were 10, 20, 40, 80, and 160 ng/μl. The surfactant was coated first, followed by ds*EpFAR*, as described in the previous section. Groups treated with ds*EGFP* (Zsyg Biotech Co. Ltd., Shanghai, China) instead of ds*EpFAR* served as the controls. The assay was performed in three replicates. The tape and mesh were also used as protection, and the lethal effect of ds*EpFAR* was assessed using the method described in the previous section. The dose that caused no significantly different mortality from the control was deemed as a tolerated dose of ds*EpFAR* and was used in the RNAi assay.

RNAi assay. We performed an RNAi assay by using a tolerated dose of ds*EpFAR* to explore the impacts of ds*EpFAR* on the expression of *EpFAR* and the development of nymphs. Newly molted second-instar nymphs, which had not yet begun to secrete waxy secretion, were used in these assays. Coating ds*EpFAR* solution on the body was selected and used after comparing and analyzing the spraying and soaking methods (Maeda et al. 2001, Tabara et al. 1998, Wang et al. 2011, Yan et al. 2020). Triton X-100 (nontoxic dose) and ds*EpFAR* (tolerated dose) were coated as described in the previous two sections. The control groups

were treated with ds*EGFP* replacing the ds*EpFAR* solution. In total, 44 groups were assigned to three treatments (each with 22 groups) and treated with ds*EpFAR* or ds*EGFP*. Double-sided adhesive tape and fine mesh were used for protective measures as described previously (Fig. 2B). From each treatment, 18 of the 22 groups with >30 nymphs per group were divided into three batches that were collected on days 2, 4, and 8 posttreatment and preserved in liquid nitrogen for the subsequent extraction of total RNA or protein. Twenty nymphs were collected from each group. The other eight groups (four groups in the ds*EpFAR* and four in the control treatments) with >60 nymphs per group were allowed to continue infesting the hosts, and their phenotypic characterizations, including wax secretion, weight gain, and pupation, were calculated at the end of the experiment.

Analysis of efficiency of interference. The level of transcription of *EpFAR* in nymphs treated with ds*EpFAR* was determined using a real-time quantitative reverse-transcription PCR (qRT-PCR). Total RNA was extracted from the whole insect body by using an EZ-10 DNAaway RNA mini-prep kit (Sangon Biotech, Shanghai, China) following the manufacturer's instructions. Next, 1 μg of RNA was reverse transcribed using an RT EasyTM II kit (Foregene, Chengdu, China) according to the manufacturer's instructions. Gene-specific primers for qRT-PCR were designed using Primer Premier 6.0 and are listed in Table 1. The qRT-PCR was performed using a CFX96 real-time PCR system (Bio-Rad) in a 20-μl reaction mixture that contained 10 μl of Universal SYBR qPCR master mix (Biosharp, Shanghai, China), 20 ng of synthesized cDNA, and 0.2 μM of forward and reverse primers. The reaction was performed under the following conditions: predenaturation at 95°C for 2 min, followed by 39 cycles of denaturation at 95°C for 15 s and annealing at 60°C for 30 s. β-Actin was used to normalize the gene expression. The experiment was conducted in three replicates. The relative level of expression of *EpFAR* was analyzed using the $2^{-\Delta\Delta Ct}$ method (Schmittgen and Livak 2008).

To investigate the effects on the EpFAR protein after the ds*EpFAR* treatment, changes in the EpFAR protein were analyzed by western blotting. The nymphs treated with ds*EpFAR* were collected on days 2, 4, and 8 after treatment. Their total protein was extracted using RIPA lysis buffer (Beyotime, Shanghai, China) following the manufacturer's instructions. The concentration of *EpFAR* was determined using an enhanced BCA protein assay kit (Beyotime). Equal proteins from different samples were fractionated by electrophoresis by using a 12% sodium dodecyl-sulfate polyacrylamide gel electrophoresis. The fractionated proteins were transferred onto nitrocellulose membranes and immunolabeled at 37°C for 1 h with a rabbit polyclonal anti-*EpFAR* antibody (1:200) as described previously (Hu et al. 2014) and incubated with horseradish peroxidase–coupled secondary antibody (1:5,000, Zoonbio Biotechnology Co., Ltd., Nanjing, China). Immunolabeling was detected using an electrogenerated chemiluminescence western blotting system (Roche, Diagnostics, Shanghai, China), with β-actin (1:5,000) as the loading control.

Phenotypic characterization of *E. pela* after RNAi. The characteristics of the secreted wax were assessed using a VHX-5000 microscopic imaging system (Keyence, Osaka, Japan) to investigate the effect of ds*EpFAR* on the ability of *E. pela* to secrete wax. Investigations were on days 2, 4, and 8 after treatment with ds*EpFAR*. To assess the cumulative impact of ds*EpFAR* on the potential to secrete wax and the development of *E. pela*, the cumulative quantity of wax, weight of the nymph,

and metamorphosis of nymphs at the end of the assay were determined when the first male adult emerged in the treatment or control groups. The numbers of molted male adults trapped in each mesh were counted. The waxy covering with nymphs and pupae was detached from the branches. All the nymphs and pupae in the waxy covering were removed using smooth tweezers. Next, the nymphs, propupae, true-pupae (True-pupa, a real pupa, its wing, leg and antennae are visible. true-pupa is different from propupa which is similar to its nymphal shape.), and male adults were separated and counted. The waxy covering and nymphs in each group were separately weighed using a high-precision balance (Mettler Toledo, Shanghai, China). This assay was replicated four times with a single group serving as a replicate.

Statistical analysis. The data were analyzed using SPSS 20.0 (IBM, Inc., Armonk, NY). For the toxicity of surfactant and ds*EpFAR*, the percent mortality was corrected by adjusting the treatment mortality with that of the control using Abbott's correction (Abbott 1925). The corrected mortality (R_{cr}) was calculated using the following formula: R_{cr} (%) = $(R_{tr} - R_{co})/(1 - R_{co}) \times 100\%$, where R_{tr} is the mortality rate of the group treated with ds*EpFAR* and R_{co} is the mortality rate of the control group. The differences in mortality were analyzed using a one-way analysis of variance, and the means were separated by a Tukey's honestly significant difference multiple comparison test ($\alpha = 0.05$). Before analysis, the variance was normalized by arcsine-square root transformation of the percentage data (Yang et al. 2020). To assess the phenotypic changes, the pupation rate (P_{pu}), the proportion of propupa (P_{pr}), and the proportion of true-pupa (P_{tr}) per group were calculated using the following formulae: P_{pu} (%) = $(N_{pr} + N_{tr} + N_{ad})/(N_{la} + N_{pr} + N_{tr} + N_{ad}) \times 100\%$; P_{pr} (%) = $N_{pr}/(N_{la} + N_{pr} + N_{tr} + N_{ad}) \times 100\%$, and; P_{tr} (%) = $(N_{tr} + N_{ad})/(N_{la} + N_{pr} + N_{tr} + N_{ad}) \times 100\%$, where N_{la}, N_{pr}, N_{tr}, and N_{ad} represent the number of nymphs, propupae, true-pupae, and adults in a group, respectively. To determine the weight of wax secreted per nymph (W_{wa}) and the weight per nymph (W_{la}), the following formulae were used: $W_{wa} = W_{wq}/(N_{la} + N_{pr} + N_{tr} + N_{ad})$ and $W_{la} = W_{tl}/N_{la}$, where W_{wq} represents the weight of wax covering secreted per group and W_{tl} represents the weight of nymphs in a group. The differences in the levels of expression of *EpFAR*, wax weights, nymphal weights, pupation rate, or the proportion of propupa and true-pupa between the study control groups compared using a Student's *t* test ($P < 0.05$). Before analysis, the rate and proportion data were transformed by arcsin $\sqrt{x}$.

Results

Nontoxic dose of surfactant. The mortality of nymphs treated with different concentrations of Triton X-100 is shown in Fig. 3A. The corrected mortality rate of the nymphs coated with 3, 1, 0.3, 0.1, and 0.03% Triton X-100 was 8.1, 3.22, 2.23, 1.48, and 0%, respectively. There was a significant difference in the mortality rates between the groups treated with Triton X-100 and the control ($F = 4.260$; df = 5, 12; $P = 0.018$). However, when the concentration of Triton X-100 was <1%, the difference between the mortality of the groups treated with Triton X-100 and the control was insignificant, suggesting that the nymphal life was not affected by Triton X-100 when the concentration of Triton X-100 was <1%. Specifically, 0.1% Triton X-100 had negligible adverse effects on the lives of *E. pela* nymphs and good affinity; thus, it was deemed as the nontoxic dose and used as the surfactant during ds*EpFAR* toxicity and RNAi assays.

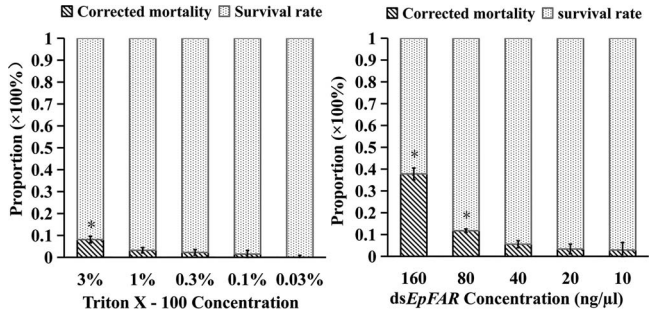

Fig. 3. Lethal effect following treatment with Triton X-100 (A) and ds*EpFAR* (B). The vertical lines represent the SEM mortality rates (*n* = 3), whereas the asterisks indicate significant differences in the mortality rates between the groups treated with ds*EpFAR* and those of the control (analysis of variance, Tukey's honestly significant difference test, $P < 0.05$).

Tolerated dose of ds*EpFAR*. The ds*EpFAR* toxicity assay revealed that 160 and 80 ng/μl ds*EpFAR* caused a relatively higher rate of nymphal mortality (37.79 and 11.76%, respectively), which was significantly different from the control (Fig. 3B; $F = 21.617$; df = 5, 12; $P < 0.0001$). However, the differences in the rates of nymphal mortality between the ds*EpFAR* and the control groups were insignificant when the ds*EpFAR* concentrations were ≤40 ng/μl. In particular, the mortality rate at 40, 20, 10 and 0 ng/μl (control) ds*EpFAR* was 4.58, 3.38, 2.91, and 4.39%, respectively. Therefore, 40 ng/μl ds*EpFAR* was deemed as the tolerated dose and used in the RNAi assay to establish the relationship between *EpFAR* and wax secretion.

Expression of *EpFAR* in nymphs treated with ds*EpFAR*. The effect of ds*EpFAR* on *EpFAR* in *E. pela* nymph is shown in Fig. 4. The relative transcription level

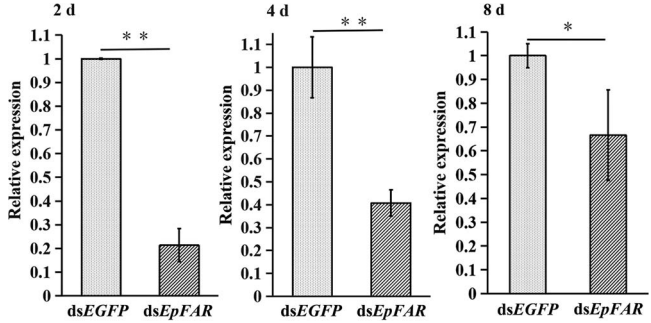

Fig. 4. Relative expression (fold) of *EpFAR* in the male nymphs at days 2, 4, and 8 after treatment with ds*EpFAR*. The error bars indicate the SEM (*n* = 3), whereas the asterisks indicate statistically significant differences between the groups treated with ds*EpFAR* and those of the control (Student's *t* test; **P* < 0.05; ***P* < 0.01).

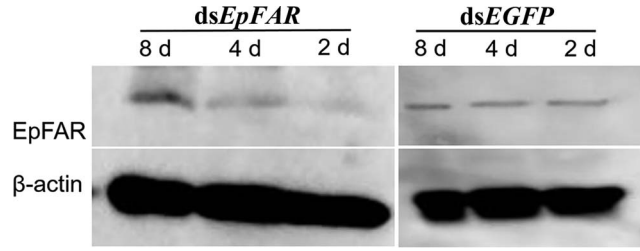

Fig. 5. Effects of ds*EpFAR* on the EpFAR protein in male nymphs at 2, 4, and 8 days posttreatment.

of *EpFAR* in the second-instar nymphs treated with ds*EpFAR* was significantly downregulated on days 2, 4, and 8 compared with the control (day 2: $t = 18.687$; $df = 4$; $P < 0.0001$; day 4: $t = 13.727$; $df = 4$; $P < 0.0001$; and day 8: $t = 4.512$; $df = 4$; $P = 0.011$). On days 2, 4, and 8, the expression of *EpFAR* was reduced by 4.69-, 2.45-, and 1.50-fold after treatment with ds*EpFAR*, respectively. The results suggest that the ds*EpFAR* can disrupt the transcript of gene *EpFAR* in *E. pela* nymph.

Ds*EpFAR* influence on accumulation of EpFAR protein. The effect of ds*EpFAR* on the EpFAR protein in *E. pela* nymph based on western blotting is summarized in Fig. 5. The EpFAR protein in the groups treated with ds*EpFAR* and the control clearly differed. The amount of EpFAR protein in the nymph treated with ds*EpFAR* was very low on days 2 and 4 after treatment. On 8 d posttreatment, the quantity of EpFAR protein in the group treated with ds*EpFAR* increased compared with that of days 2 and 4. However, the amount of EpFAR protein in the control group on days 2, 4, and 8 did not clearly vary. The level of EpFAR protein showed the variation tendency of rising after falling with time due to ds*EpFAR* treatment. The variation trend of the EpFAR protein was consistent with the change in the level of transcription of *EpFAR* in the nymphs treated with ds*EpFAR*. The results suggest that ds*EpFAR* can disrupt the expression of EpFAR protein.

Wax secretion capability after ds*EpFAR* treatment. To evaluate the influence of RNAi on wax secretion, the changes in wax secretion were recorded at different times and the cumulative wax during the assay period was also evaluated. On day 2 posttreatment, the wax secretion feature of the nymphs treated with ds*EpFAR* was similar to that of the control, with only very little wax "powder" on the nymphal body surface (Fig. 6). On 4 d posttreatment, a little wax filament was sparsely scattered on the nymphal body surface and a clump of wax filament on the side of the thorax was visible in the group treated with ds*EpFAR*. By contrast, a layer of wax filament covered the backs of nymphs in the ds*EGFP*-treated group, which obscured the the nymphal body. On day 8 posttreatment, the nymphs in the groups treated with ds*EpFAR* remained visible, although there was a slight increase in the wax filament compared with those at 4 d. However, a very dense layer of wax filament, named wax quilt, had entirely covered the nymphs in the ds*EGFP*-treated group on day 8 posttreatment. The results suggest that the nymphs cannot normally secrete wax after ds*EpFAR* treatment.

The cumulative wax was collected and weighed at the end of the RNAi assay. The maximum weight of fresh wax secreted by each nymph in the ds*EpFAR* treatment

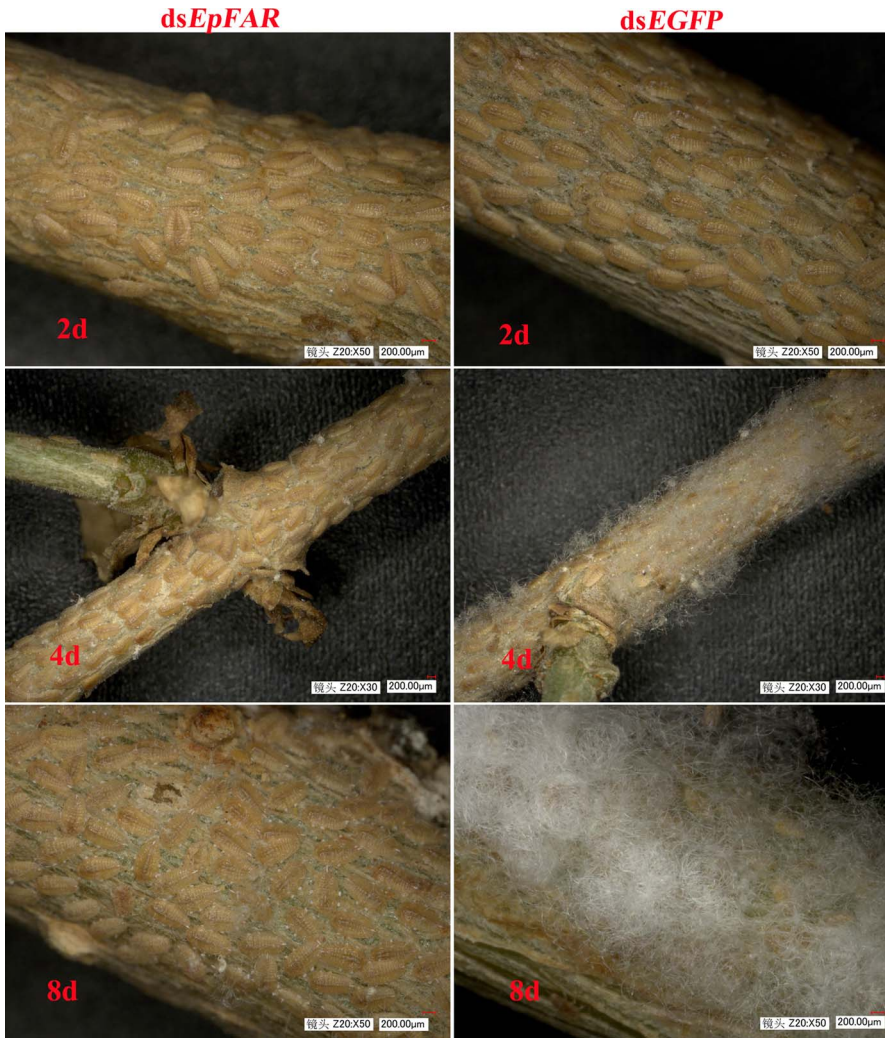

Fig. 6. Wax secretion of *Ericerus pela* at days 2, 4, and 8 after treatment with ds*EpFAR*. 2d: amount of wax both in ds*EpFAR* group and ds*EGFP* group is comparable; 4d: a little wax filament was visible in ds*EpFAR* group, but in ds*EGFP* group, there was a layer of wax filament; 8d: some wax filament is on the body surface in ds*EpFAR* group, but in ds*EGFP* group, there was so much wax that the body of nymph was invisible.

group was 0.359 mg/♂ and the minimum weight was 0.305 mg/♂, with an average weight of 0.341 mg/♂, which was significantly lower than that of the control with an average weight of 0.409 mg/♂ ($t = 2.458$; df $= 6$; $P = 0.049$). These results imply a weakened capability of wax secretion for the ds*EpFAR*-treated nymphs (Fig. 7).

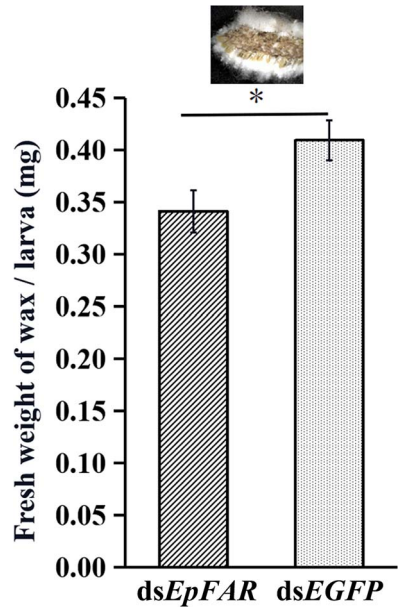

Fig. 7. Effects of ds*EpFAR* on the cumulative wax per nymph. The error bars represent the SEM (*n* = 4), whereas the asterisks indicate statistically significant differences between the groups treated with ds*EpFAR* and the control groups (Student's *t* test; **P* < 0.05).

Effects of ds*EpFAR* on growth and development of *E. pela*. To investigate the effects of *EpFAR* interference on the growth and development of *E. pela*, the weight of nymphs was examined at the end of the RNAi assay. The male nymphs of *E. pela* treated with ds*EpFAR* weighed 0.28 mg/nymph, on average, whereas the control weight was 0.32 mg (Fig. 8A), which was significantly different ($t = 2.806$; df = 6; $P = 0.031$). The results suggest that ds*EpFAR* inhibited the growth of male nymphs.

Interestingly, the uptake of ds*EpFAR* significantly affected the rate of nymphal pupation with 24% of those treated with ds*EpFAR* ($t = 5.522$; df = 6; $P = 0.001$). However, in the control group, the pupation rate was 5.7% where most individuals were in the immature stage and secreting wax. Furthermore, the rate of emergence of true-pupae from the groups treated with ds*EpFAR* was higher than that of the control ($t = 4.348$; df = 6; $P = 0.005$). In particular, the ratio of true-pupae to total pupae in the group treated with ds*EpFAR* was 3.16-fold higher than that in the ds*EGFP*-treated group (Fig. 8B). Indeed, in the process of experiment, the first male adult emerged from the group treated with ds*EpFAR*, and no male adult was observed in the ds*EGFP*-treated group until the end of the assay. The significant difference in the pupation rate showed that the nymphs treated with ds*EpFAR* entered the pupal stage earlier than what is customary, suggesting the ds*EpFAR* affected the development of the nymphs. From another point of view, the early pupation implied that the period of feeding damage in the life of male *E. pela* was clearly shortened compared with that of the control.

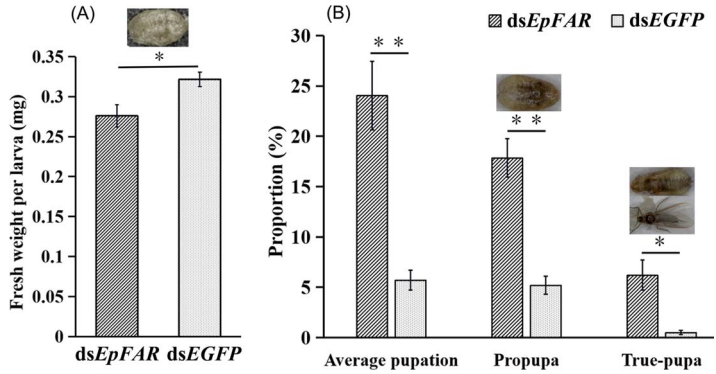

Fig. 8. Effects of ds*EpFAR* on the nymphal growth and development. (A) Net weight gain per nymph. (B) Pupation rate and the proportion of propupa and true-pupa. The error bars represent the SEM (*n* = 4), whereas the asterisks indicate statistically significant differences between the groups treated with ds*EpFAR* and the control groups (Student's *t* test; **P* < 0.05; ***P* < 0.01).

Discussion

Ericerus pela is a forestry pest in most regions of China, except southwestern China. The broad-leaved forest and urban green land with glossy privets and ash trees as the main tree species are severely damaged by this pest. The affected glossy privets and ash trees are covered with white wax that seriously affects photosynthesis and causes tree mortality. The male nymphs have no sclerotized cuticle and are highly dependent on the waxy covering to protect them from harmful biotic and abiotic factors. Interrupting the synthesis of wax presented an intriguing approach to the management of *E. pela*. It was confirmed that dsRNA can kill the pest based on destroying the function of target gene, and its success greatly depends on suitable target genes (Dhandapani et al. 2020, Luo et al. 2017, Wang et al. 2021a). RNAi also can affect the development of pests because some loss-of-function phenotypes were generated through a depletion of chosen transcript (Bellés 2010, Jain et al. 2020). In this study, by using the RNAi technology, we unveiled the role of *EpFAR*, with the results showing promise for RNAi-based *E. pela* management.

FARs are the key enzymes in the biosynthesis of fatty alcohols, which are precursors of wax esters, cuticular hydrocarbons, and sex pheromones in some insects (Dou et al. 2020, Finet et al. 2019, Li et al. 2019). For *E. pela*, the downregulation of *EpFAR* conspicuously decreased the wax secretion within the first 8 d, followed by a significant decrease in the cumulative wax at the end of the trial. This suggested that *EpFAR* is essential for the biosynthesis of wax. The wax, as is known to all, has a function as a protective barrier for insects. So, once the wax on the surface of the body of *E. pela* decreases due to ds*EpFAR* treatment, *E. pela* probably loses an effective protective barrier that is potentially fatal to *E. pela*. During the process of experiment, there appeared to be a slight increase in the relative expression level of *EpFAR* after day 8 posttreatment, which might be induced by

the degradation of ds*EpFAR* due to some unknown factors. Regardless, there was *EpFAR* interference and the secretion of wax was decreased, which was helpful for further research of ds*EpFAR*.

Larval weight is generally a health indicator, and weight loss is associated with abnormal larval development. Luo et al. (2017) reported a series of changes in female *A. suturalis* following the downregulation of *AsFAR* at day 0 posteclosion, including a significant decline in the number of oocytes, dry weight of ovaries, lifetime fecundity, and egg hatchability. Adult weight and number of eggs laid by *L. decemlineata* adults fed on plant-derived dsRNA as larvae were decreased (Guo et al. 2018). In our study, the fresh nymphal weight in the group treated with ds*EpFAR* significantly decreased, suggesting that the nutrition metabolism of *E. pela* was likely interrupted by ds*EpFAR*. Therefore, it can be concluded that *EpFAR* is related to the development and growth of *E. pela* and that ds*EpFAR* is a severe threat to the nymphal health.

In this study, ds*EpFAR* accelerated the metamorphosis of *E. pela* nymphs: many treated nymphs entered the pupal stage earlier than those in the natural process. In addition, the proportion of true-pupa in the group treated with ds*EpFAR* was higher than that in the control, implying that pupation in the group treated with ds*EpFAR* took place earlier than in the control. The precocious metamorphosis suggested that the developmental duration of male nymphs was shortened, possibly due to their abnormal growth and development. Phenotypic changes under gene deficiency induced by dsRNA have been observed in other insects, such as precocious metamorphosis in *Tribolium castaneum* (Herbst) (Coleoptera: Tenebrionidae) and *L. decemlineata* (Guo et al. 2018, Minakuchi et al. 2008); smaller basal oocytes in *Schistocerca gregaria* Forsskål (Orthoptera: Acrididae) induced by the knockdown of specific genes (Marchal et al. 2011); malformed oocytes caused by ds*NlFAR4*, ds*NlFAR6*, and ds*NlFAR9* in the brown planthopper (*Nilaparvata lugens* (Stål)) (Li et al. 2020); and altered microstructure of the epicuticle layer due to the knockdown of *NlFAR* in *N. lugens* (Li et al. 2019). In addition, the available evidence also indicated that typical phenotypes of specific gene deficiency and sensitivity to RNAi are different among insect species (Christiaens et al. 2014, Coleman et al. 2015, Zhang et al. 2015). In this study, the *E. pela* nymphs pupated earlier because of ds*EpFAR*, which shortened the period of damage to the host. Because phenotypic abnormality significantly influenced individual vitality, successful interference with *EpFAR* will effectively lower population viability.

An important challenge for most insect RNAi studies, especially for the future application of dsRNA for pest control practice, is developing a delivery method. Thus far, two dsRNA application methods are being developed: host-induced gene silencing wherein the host plant is engineered to express the dsRNA molecules and spray-induced gene silencing (SIGS) that avoids the challenges surrounding the regulation of genetic modification (Wytinck et al. 2020). SIGS using naked dsRNA has been shown to be an effective control method against some insect pests (Killiny et al. 2014, Zhang et al. 2020). Among the SIGS methods, the soaking method is a classical method successfully applied to the nematode *Caenorhabditis elegans* (Maupas) (Tabara et al. 1998). The epidermal microapplication of dsRNA also successfully induced interference of the target genes in the Asian citrus psyllid *Diaphorina citri* Kuwayama (Hemiptera: Liviidae) (El-Shesheny

et al. 2013). In some reports, nanoparticles, cell-penetrating peptides, or cationic liposomes were applied in the laboratory or greenhouse environment with the goal of decreasing the degradation of dsRNA, although they can partly increase the possibility of dsRNA delivery (Adams et al. 2019, Chen et al. 2012, Joga et al. 2016, Lin et al. 2017, Milletti 2012, Zhou et al. 2015). However, the production costs of these dsRNA carriers and the economic cost of RNAi-based technologies exceed levels deemed appropriate for the wide-scale field use (Zotti et al. 2018). In our study, these newly molted nymphs measure only 0.78 $\times$ 0.43 mm and are fixed on host plant branches, both factors limiting application by injection. We found that the epidermal application of dsRNA by using the soaking methods coated the bodies of newly molted nymphs with the ds*EpFAR* solution. We also found that this coating must remain in place for 60 s for the ds*EpFAR* to infiltrate the epidermis as much as possible. At this point, the newly molted nymphs have not yet begun to secrete waxy secretion and they are likely more sensitive to the dsRNA than those at older stages of development. Furthermore, wax glands are present on nymph epidermis and it has been confirmed that the gene *EpFAR* is expressed mainly in wax glands (Hu et al. 2018).

Pest management of scale insects typically targets females, which contrasts with the management of *E. pela* where males are the key targets. The fecundity of female *E. pela* is naturally high, with the female-to-male ratio being 1:4. The male nymphs comprise a very large percentage of the total *E. pela* population; therefore, limiting the number of male *E. pela* could significantly reduce the damage they cause to infested plants. Nevertheless, given the relationship between population and female fertility, it is necessary to explore the role of *EpFAR* in female *E. pela* in the future.

Acknowledgment

This work was supported by the National Natural Science Foundation of China under grant U1804104.

References Cited

Abbott, W.S. 1925. A method of computing the effectiveness of an insecticide. J. Econ. Entomol. 18: 265–267.

Adams, S., P. Pathak, H. Shao, J.B. Lok and A. Pires-da Silva. 2019. Liposome-based transfection enhances RNAi and CRISPR-mediated mutagenesis in non-model nematode systems. Sci. Rep. 9: 483.

Bellés, X. 2010. Beyond *Drosophila*: RNAi in vivo and functional genomics in insects. Annu. Rev. Entomol. 55: 111–128.

Bosher, J.M. and M. Labouesse. 2000. RNA interference: Genetic wand and genetic watchdog. Nat. Cell Biol. 2: E31–E36.

Chen, X.M. 2011. Natural Population Ecology of *Ericerus pela*. Science Press, Beijing.

Chen, Y.J., B.R. Liu, Y.H. Dai, C.Y. Lee, M.H. Chan, H.H. Chen, H.J. Chiang and H.J. Lee. 2012. A gene delivery system for insect cells mediated by arginine-rich cell-penetrating peptides. Gene 493: 201–210.

Cheng, J.B. and D.W. Russell. 2004. Mammalian wax biosynthesis I. Identification of two fatty acyl-coenzyme A reductases with different substrate specificities and tissue distributions. J. Biol. Chem. 279: 37789–37797.

Christiaens, O., L. Swevers and G. Smagghe. 2014. DsRNA degradation in the pea aphid (*Acyrthosiphon pisum*) associated with lack of response in RNAi feeding and injection assay. Peptides 53: 307–314.

Coleman, A.D., R.H.M. Wouters, S.T. Mugford and S.A. Hogenhout. 2015. Persistence and transgenerational effect of plant-mediated RNAi in aphids. J. Exp. Bot. 66: 541–548.

Dang, C., Y. Zhang, C. Sun, R. Li, F. Wang, Q. Fang, H. Yao, D. Stanley and G. Ye. 2022. dsRNAs targeted to the brown planthopper *Nilaparvata lugens*: Assessing risk to a non-target, beneficial predator, *Cyrtorhinus lividipennis*. J. Agric. Food Chem. 70: 373–380.

Dhandapani, R.K., D. Gurusamy, J.J. Duan and S.R. Palli. 2020. RNAi for management of Asian long-horned beetle, *Anoplophora glabripennis*: Identification of target genes. J. Pest Sci. 93: 823–832.

Ding, W.F., X.F. Ling, Q. Lu, W.W. Wang, X. Zhang, Y. Feng, X.M. Chen and H. Chen. 2022. Identification of the key pathways and genes involved in the wax biosynthesis of the Chinese white wax scale insect (*Ericerus pela* Chavannes) by integrated weighted gene coexpression network analysis. Genes 13: 1364.

Dou, X., A. Zhang and R. Jurenka. 2020. Functional identification of fatty acyl reductases in female pheromone gland and tarsi of the corn earworm, *Helicoverpa zea*. Insect Biochem. Mol. 116: 103260.

El-Shesheny, I., S. Hajeri, I. El-Hawary, S. Gowda and N. Killiny. 2013. Silencing abnormal wing disc gene of the Asian citrus psyllid, *Diaphorina citri* disrupts adult wing development and increases nymph mortality. PloS One 8: e65392.

Finet, C., K. Slavik, J. Pu, S.B. Carroll and H. Chung. 2019. Birth-and-death evolution of the fatty acyl-CoA reductase (FAR) gene family and diversification of cuticular hydrocarbon synthesis in *Drosophila*. Genome Biol. Evol. 11: 1541–1551.

Guo, W., C. Bai, Z. Wang, P. Wang, Q. Fan, X. Mi, L. Wang, J. He, J. Pang, X. Luo, W. Fu, Y. Tian, H. Si, G. Zhang and J. Wu. 2018. Double-stranded RNAs high-efficiently protect transgenic potato from *Leptinotarsa decemlineata* by disrupting juvenile hormone biosynthesis. J. Agric. Food Chem. 66: 11990–11999.

Hu, Y., X. Chen, P. Yang and W. Ding. 2018. Characterization and functional assay of a fatty acyl-CoA reductase gene in the scale insect, *Ericerus pela* Chavannes (Hemiptera: Coccoidae). Arch. Insect Biochem. 97: e21445.

Hu, Y., P. Yang, X. Chen and D. Xu. 2014. Preparation of polyclonal antibody against *Ericerus pela* FAR peptide. Fore. Res. 27: 82–85.

Jain, R.G., K.E. Robinson, S.J. Fletcher and N. Mitter. 2020. RNAi-based functional genomics in Hemiptera. Insects 11: 557.

Jaspers, M.H.J., R. Pflanz, D. Riedel, S. Kawelke, I. Feussner and R. Schuh. 2014. The fatty acyl-CoA reductase Waterproof mediates airway clearance in *Drosophila*. Dev. Biol. 385: 23–31.

Joga, M.R., M.J. Zotti, G. Smagghe and O. Christiaens. 2016. RNAi efficiency, systemic properties, and novel delivery methods for pest insect control: What we know so far. Front. Physiol. 17: 553.

Killiny, N., S. Hajeri, S. Tiwari, S. Gowda and L.L. Stelinski. 2014. Double-stranded RNA uptake through topical application, mediates silencing of five CYP4 genes and suppresses insecticide resistance in *Diaphorina citri*. PloS One 9: e110536.

Li, D., X. Chen, X. Wang and C. Zhang. 2019. FAR gene enables the brown planthopper to walk and jump on water in paddy field. Sci. China Life Sci. 62: 1521–1531.

Li, D., Y. Dai, X. Chen, X. Wang, Z. Li, B. Moussian and C. Zhang. 2020. Ten fatty acyl-CoA reductase family genes were essential for the survival of the destructive rice pest, *Nilaparvata lugens*. Pest Manag. Sci. 76: 2304–2315.

Lin, Y.H., J.H. Huang, Y. Liu, X. Belles and H.J. Lee. 2017. Oral delivery of dsRNA lipoplexes to German cockroach protects dsRNA from degradation and induces RNAi response. Pest Manag. Sci. 73: 960–966.

Luo, J., S. Liang, J. Li, Z. Xu, L. Li, B. Zhu, Z. Li, C. Lei, K. Lindsey, L. Chen, S. Jin and X. Zhang. 2017. A transgenic strategy for controlling plant bugs (*Adelphocoris suturalis*)

through expression of double-stranded RNA homologous to fatty acyl-coenzyme A reductase in cotton. New Phytol. 215: 1173–1185.

Maeda, I., Y. Kohara, M. Yamamoto and A. Sugimoto. 2001. Large-scale analysis of gene function in *Caenorhabditis elegans* by high-throughput RNAi. Curr. Biol. 11: 171–176.

Marchal, E., J. Zhang, L. Badisco, H. Verlinden, E.F. Hult, P. Van Wielendaele, K.J. Yagi, S.S. Tobe and J.V. Broeck. 2011. Final steps in juvenile hormone biosynthesis in the desert locust, *Schistocerca gregaria*. Insect Biochem. Mol. 41: 219–227.

Milletti, F. 2012. Cell-penetrating peptides: Classes, origin, and current landscape. Drug Discov. 17: 850–860.

Minakuchi, C., T. Namiki, M. Yoshiyama and T. Shinoda. 2008. RNAi-mediated knockdown of juvenile hormone acid O-methyltransferase gene causes precocious metamorphosis in the red flour beetle *Tribolium castaneum*. FEBS J. 275: 2919–2931.

Munkajohnpong, P., C. Kesornpun, S. Buttranon, J. Jaroensuk, N. Weeranoppanant and P. Chaiyen. 2020. Fatty alcohol production: an opportunity of bioprocess. Biofuel Bioprod. Biorefin. 14: 986–1009.

Palli, S.R. 2014. RNA interference in Colorado potato beetle: Steps toward development of dsRNA as a commercial insecticide. Curr. Opin. Insect Sci. 6: 1–8.

Schmittgen, T.D. and K.J. Livak. 2008. Analyzing real-time PCR data by the comparative CT method. Nat. Protoc. 3: 1101–1108.

Tabara, H., A. Grishok and C.C. Mello. 1998. RNAi in *C. elegans*: Soaking in the genome sequence. Science 282: 430–431.

Teerawanichpan, P. and X. Qiu. 2010. Fatty acyl-CoA reductase and wax synthase from *Euglena gracilis* in the biosynthesis of medium-chain wax esters. Lipids 45: 263–273.

Tian, G., L. Cheng, X. Qi, Z. Ge, C. Niu, X. Zhang and S. Jin. 2015. Transgenic cotton plants expressing double-stranded RNAs target HMG-CoA reductase (HMGR) gene inhibits the growth, development and survival of cotton bollworms. Int. J. Biol. Sci. 11: 1296–1305.

Tong, H., Y. Wang, S. Wang, M.A.A. Omar, Z.C. Li, Z.H. Li, S. Ding, Y. Ao, Y. Wang, F. Li and M. Jiang. 2022. Fatty acyl-CoA reductase influences wax biosynthesis in the cotton mealybug, *Phenacoccus solenopsis* Tinsley. Commun. Biol. 5: 1108.

Wang, H.D. and H.Y. Wang. 2014. Damage of *Ericerus pela* and control strategy. J. Liaoning For. Sci. Technol. 3: 80–82.

Wang, K., H. Cheng, J. Chen, G. Zhu, P. Tang and Z. Han. 2021a. Chimeric double-stranded RNAs could act as tailor-made pesticides for controlling storage insects. J. Agric. Food Chem. 69: 6166–6171.

Wang, Y., Y. Sun, Q. You, W. Luo, C. Wang, S. Zhao, G. Chai, T. Li, X. Shi, C. Li, R. Jetter and Z. Wang. 2018. Three fatty acyl-coenzyme a reductases, BdFAR1, BdFAR2 and BdFAR3, are involved in cuticular wax primary alcohol biosynthesis in *Brachypodium distachyon*. Plant Cell Physiol. 59: 527–543.

Wang, Y., J. Xu, Z. He, N. Hu, W. Luo, X. Liu, X. Shi, T. Liu, Q. Jiang, P. An, L. Liu, Y. Sun, R. Jetter, C. Li and Z. Wang. 2021b. BdFAR4, a root-specific fatty acyl-coenzyme A reductase, is involved in fatty alcohol synthesis of root suberin polyester in *Brachypodium distachyon*. Plant J. 106: 1468–1483.

Wang, Y., H. Zhang, H. Li and X. Miao. 2011. Second-generation sequencing supply an effective way to screen RNAi targets in large scale for potential application in pest insect control. PloS One 6: e18644.

Wynant, N., D. Santos and J.V. Broeck. 2014. Biological mechanisms determining the success of RNA interference in insects. Int. Rev. Cel. Mol. Biol. 312: 139–167.

Wytinck, N., C.L. Manchur, V.H. Li, S. Whyard and M.F. Belmonte. 2020. dsRNA uptake in plant pests and pathogens: Insights into RNAi-based insect and fungal control technology. Plants 9: 1780.

Yan, S., J. Qian, C. Cai, Z. Ma, J. Li, M. Yin, B. Ren and J. Shen. 2020. Spray method application of transdermal dsRNA delivery system for efficient gene silencing and pest control on soybean aphid *Aphis glycines*. J. Pest Sci. 93: 449–459.

Yang, Y.J., C.Y. Wang, H.X. Xu, J.C. Tian and Z.X. Lu. 2020. Response of *Trichogramma* spp. (Hymenoptera: Trichogrammatidae) to insecticides at concentrations sublethal to *Cnaphalocrocis medinalis* (Lepidoptera: Pyralidae). J. Econ. Entomol. 113: 646–653.

Zhang, J., S.A. Khan, C. Hasse, S. Ruf, D.G. Heckel and R. Bock. 2015. Full crop protection from an insect pest by expression of long double-stranded RNAs in plastids. Science 347: 991–994.

Zhang, K., J. Wei, K. E. Huff Hartz, M.J. Lydy, T.S. Moon, M. Sander and K.M. Parker. 2020. Analysis of RNA interference (RNAi) biopesticides: Double-stranded RNA (dsRNA) extraction from agricultural soils and quantification by RT-qPCR. Environ. Sci. Technol. 54: 4893–4902.

Zhang, S. and C. Guo. 2018. *Ericerus pela* outbreak and control in non-production areas of white wax. Agric. Sci. Technol. 21: 121–123.

Zhou, Z., Y. Li, C. Yuan, Y. Zhang and L. Qu. 2015. Bendena, B. Oral administration of TAT-PTD-diapause hormone fusion protein interferes with *Helicoverpa armigera* (Lepidoptera: Noctuidae) development. J. Insect Sci. 15: 2–7.

Zotti, M., E.A. Dos Santos, D. Cagliari, O. Christiaens, C.N.T. Taning and G. Smagghe. 2018. RNA interference technology in crop protection against arthropod pests, pathogens and nematodes. Pest Manag. Sci. 74: 1239–1250.